Computers and Concrete, Vol. 4, No. 6 (2007) 457-475
DOI: http://dx.doi.org/10.12989/cac.2007.4.6.457

Nonlinear analysis of RC beams based on simplified moment-curvature relation considering fixed-end rotation

Sun-Pil Kim†

Hyundai Development Institute of Construction Technology, #102-4, Mabuk-Dong, Giheung-Gu, Yongin-Si, Gyounggi-Do, 446-716, Korea

(Received March 10, 2007, Accepted October 11, 2007)

Abstract. A simple analytical procedure to analyze reinforced concrete (RC) beams with cracked section is proposed on the basis of the simplified moment-curvature relations of RC sections. Unlike previous analytical models which result in overestimation of stiffness and underestimation of structural deformations induced from assuming perfect-bond condition between steel and concrete, the proposed analytical procedure considers fixed-end rotation caused by anchorage. Furthermore, the proposed analytical procedure, compared with previous numerical models, promotes effectiveness of analysis by reflecting several factors which can influence nonlinearity of RC structure into the simplified moment-curvature relation. Finally, correlation studies between analytical and experimental results are conducted to establish the applicability of the proposed analytical procedure to the nonlinear analysis of RC structures.

Keywords: reinforced concrete; anchorage slip; fix-end rotation; moment-curvature relation.

1. Introduction

Since the structural behavior of reinforced concrete (RC) structures represents complex features according to the variation of numerous influencing factors including concrete cracking, nonlinear properties of concrete, and yielding of reinforcing steel, an accurate prediction of nonlinear responses in RC structures requires an exact consideration of these nonlinear effects. However, this is time consuming and makes the nonlinear analysis of an entire structure impossible. Nevertheless, in recent years, increasing need for the assessment of the strength and serviceability of existing structures and newly designed critical structures has encouraged the application of nonlinear analysis and, in advance, the development of advanced analytical methods capable of representing the cracked behavior of RC structures under all possible loading conditions.

Material nonlinear analyses of RC beams that comprise the primary members of RC structures are generally conducted by using one of two basically different approaches: (1) the layered section approach (see Fig. 1); and (2) the modified stiffness approach (see Fig. 2). The former is based on the idealized stress-strain relations for concrete and reinforcing steel in which a finite element is divided into imaginary concrete and steel layers in a section (Kwak and Kim 2004). This approach has been broadly used by many previous investigators (Park, *et al.* 1972, Taucer, *et al*. 1991, Kwak, *et al*. 2006). However, application of this approach to large structures with many degrees of

† E-mail: kspil@hdec.co.kr

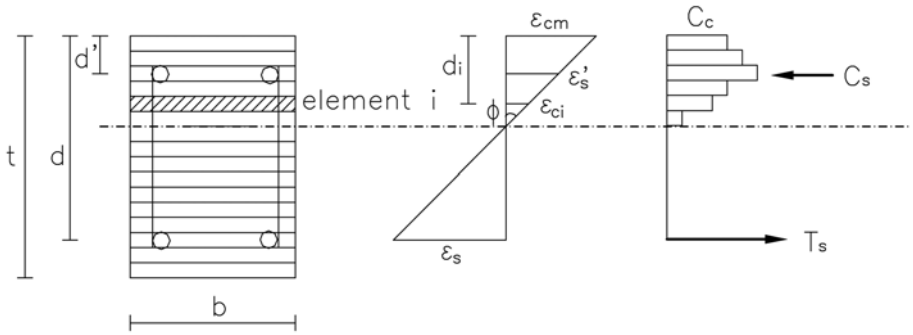

Fig. 1 Layered section approach

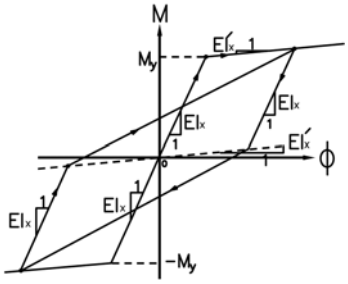

Fig. 2 Modified stiffness approach

freedom has some limitations, because numerical integrations and prediction of material states must be conducted through entire imaginary layers and stiffness of structures is usually overestimated ignoring anchorage slip of main bar at the beam-column joint. The modified stiffness approach, the other hand, is based on an overall simplified moment-curvature relation reflecting the various stages of material behavior (Clough and Johnston 1966, Roufaiel and Meyer 1987, Takeda, *et al*. 1970). In this approach, the stiffness is determined as the slope of the moment-curvature relation which is constructed by section analysis and a nonlinear analysis of RC beams can be conducted based on this moment-curvature relation. Therefore, this method, in comparison with layered section approach, can reduce calculation time and storage space in nonlinear analysis of RC beam. Nevertheless, this approach established to date still have limitations to simulate the structural behavior of RC structures because of the exclusion of fixed-end rotation effect caused by the anchorage-slip in beam-column joint.

To address these limitations, an improved nonlinear approach is introduced in this paper on the basis of the simplified moment-curvature relation of RC sections, which is uniquely defined according to the dimensions of the concrete section, the material properties of concrete and steel and axial force. In addition, to simulate the concentrative deformation at the beam-column joint, equivalent stiffness (EI_{eq}) in the plastic hinge length is introduced in the finite element formulation. Finally, validity of the proposed algorithm is established by comparing the analytical predictions with experimental results and previous analytical studies.

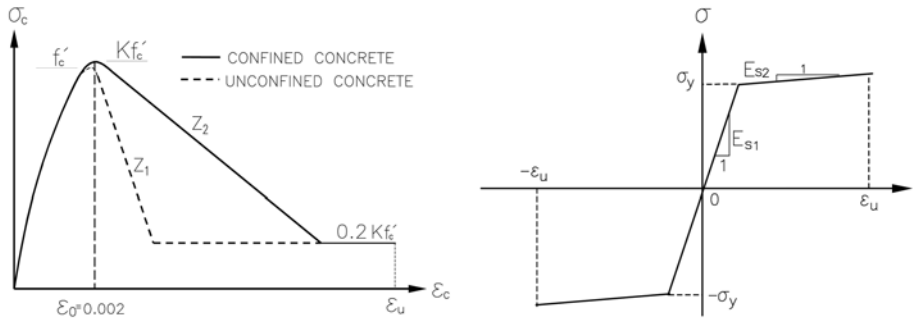

Fig. 3 Stress-strain relation

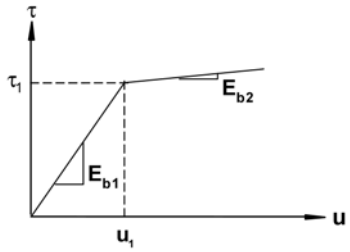

Fig. 4 Bond stress-slip relation

2. Material models

To accomplish section analysis to define moment-curvature relation, material models for concrete and steel must be defined previously. Many mathematical models for concrete are currently used in the analysis of RC structures. Among these models, the monotonic envelope curve introduced by Kent and Park and later extended by Scott, *et al.* (1982) is adopted in this study for a layered section approach for its simplicity and computational efficiency. In this model, as shown in Fig. 3(a), the monotonic concrete stress-strain relation in the compression region is described by three regions. However, the stress-strain relation in the tensile region is ignored in strength calculations in this study, because concrete has low tensile strength, generally less than 20% of the compressive strength, and it makes a negligibly small contribution to the strength and energy absorbtion capacity of an cracked RC section. Reinforcing steel is modeled as a linear elastic, linear strain hardening material with yield stress σ_y, as shown in Fig. 3(b). The reasons for this approximation are: (1) computational convenience of the model; and (2) the behavior of RC members is greatly affected by the yielding of reinforcing steel. It is, therefore, advisable to take advantage of the strain-hardening behavior of steel in improving the numerical stability of the solution. More details for the material models for concrete and steel can be found elsewhere (Kwak and Filippou 1990, Kwak and Kim 2001, Kwak and Kim 2002a, Kwak and Kim 2002b).

In contrast to the concrete and steel whose material properties are uniquely defined, the bond stress-slip relation depends on the relative deformation of concrete and steel. As well known, the relation between bond stress and slip depend on many factors including location, surface condition,

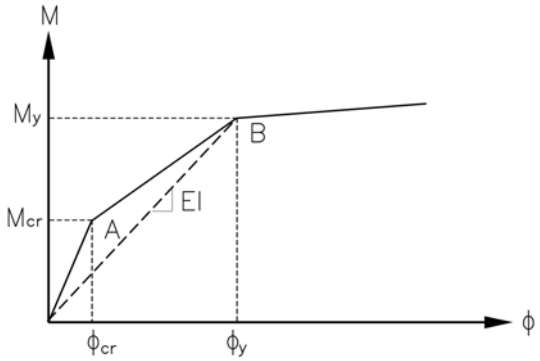

Fig. 5 Typical moment-curvature relation of RC section

and load step and so on. Therefore, it is practically impossible to establish a local bond stress-slip relation. Concurrently, average bond stress-slip relation which is measured over equal to five bar diameter is used. Moreover, the result is very sensitive to experimental error because the bond stress is derived from the change in steel stress, and the bond-slip relation also depends on the position of the bars, the surface condition of the bars, the loading stage, the boundary conditions and the anchorage length of the bars. In spite of these difficulties, several experimental bond-stress slip relations have been proposed (Ayoub and Filippou 1999, Eligehausen, *et al*. 1983, Hayashi and Kokusho 1985, Monti, *et al*. 1997). In this study, the simple bilinear bond stress-slip model (Ayoub and Filippou 1999) in Fig. 4 is adopted, and the parameters (u_1 = 0.1 cm, τ_1 = 14.85 Mpa) used in the model are obtained from experimental studies. This model gives good approximation of the actual behavior for cases that do not exhibit significant bond-slip and associated bond damage.

3. Basic moment-curvature relation

To ensure ductile behavior in practice, steel contents less than the balanced design value are always used for flexural members. The typical moment-curvature relation for a lightly reinforced concrete section with one top and one bottom layer of reinforcing steel (under-reinforced concrete section) can be idealized to the trilinear relation shown in Fig. 5. The first stage is to the cracking (point A in Fig. 5), the second to yield of the tension steel (point B in Fig. 5), and the third to the limit of useful strain in the concrete.

Up to first cracking at the extreme tension fiber, the entire cross section is effective for the applied internal moment, and the stress-strain relations for concrete and steel maintain linear elasticity. If the dimensions of the concrete section and the steel areas and positions are given, the cracking moment M_{cr} and the corresponding curvature ϕ_{cr} (point A in Fig. 5) can be calculated using the requirements of strain compatibility and equilibrium of forces. However, in this paper, this step can be abbreviated because only cracked section is dealt with.

The moment and curvature at first yield of the tensile steel (point B in Fig. 5) should also be calculated using the defined stress-strain relations for concrete and steel. Based on normal force equilibrium, a section analysis is carried out by first assuming that the tension steel reaches the yielding point. With an assumed neutral axis depth, the internal tension T and compression C can be calculated. Through successive iteration until the difference between the tensile force and compressive

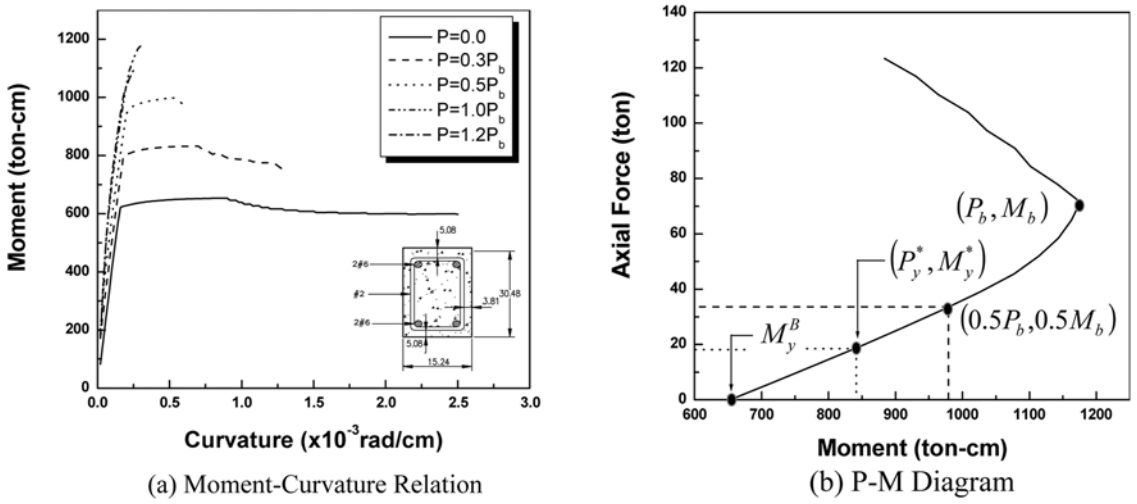

(a) Moment-Curvature Relation (b) P-M Diagram

Fig. 6 Axial force effect on moment-curvature relation

force is less than the given tolerance, the moment and curvature at steel yielding are finally determined. The connection from initial point to yield point gives the simplified basic moment-curvature relation defined in this paper. In advance, the moment-curvature relation to the post-yielding stage is approximated as a straight line which conserves same energy until ultimate point.

4. Modification of basic moment-curvature relation

4.1. Axial force effect

An axial force has an important effect on the moment-curvature relation of a RC section. Fig. 6 shows the moment-curvature relations corresponding to various levels of axial force. Up to reaching the balanced axial force P_b, the yield moment of a section increases in proportion to the axial load P and the failure curvature considerably decreases by the presence of the axial load. In particular, the application of large seismic loads acting horizontally requires an RC column to resist a load combination of a relatively small axial load and large moment. Generally, a load combination of (P, M) will be located in a region upper-bounded by the axial load of $0.5P_b$ at a $P-M$ interaction diagram, where P_b is the balanced axial force(see Fig. 6).

To implement the axial force effect into a moment-curvature relation, a linear interpolation between two boundary points of (0, M_y^B) and ($0.5P_b$, $0.5\ M_b$) is used on the basis of the assumption that the moment capacity is linearly proportional to the applied axial load P until P reaches to $0.5\ P_b$ (see Fig. 7). In reality, the axial force acting on an RC column continually changes when a frame structure is subjected to horizontal load, because lateral drift accompanying the floor rotation will occur. An accurate calculation of structural response may require taking into account this axial force variation. Nevertheless, this effect is not considered in this paper because its variation is expected to be very small in a real structure. Since most floor rotation will be prevented by a rigid floor and a strong column-weak beam system, variation of axial force will be immaterial as compared with axial force by dead load and super-imposed dead loads.

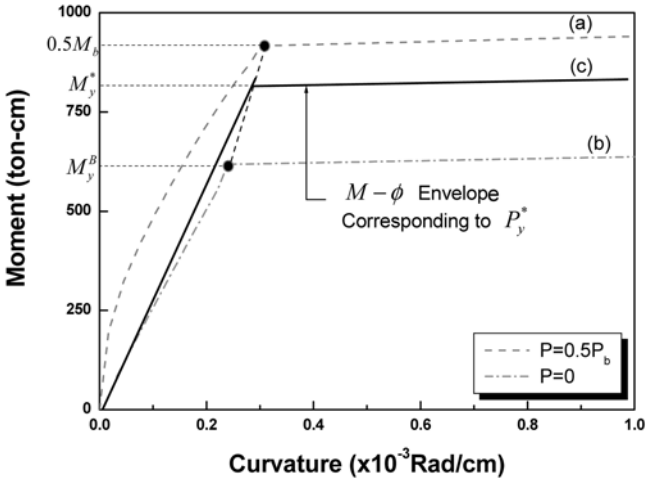

Fig. 7 Modification of moment-curvature relation considering axial force effect

4.2. Anchorage-slip effect

Since bond stresses in RC structures arise from changes in the steel stress along the length, the influence of bonding becomes more pronounced in a cracked region. In a simplified analysis of RC structures, complete compatibility of strains between concrete and steel is usually assumed, which implies a perfect bond condition. However, this assumption is realistic only in regions where negligible stress transfer between the two components takes place. In regions of high transfer stresses along the interface between reinforcing steel and surrounding concrete, such as near cracks, the bond stress is related to the relative displacement between reinforcing steel and concrete. Therefore, the bond-slip effect must also be considered to simulate the structural behavior more exactly. In this regard, many studies have been carried out to simulate this effect based on finite element analysis (Ayoub and Filippou 1999, Monti, *et al*. 1997a, 1997b) and experimental results (Eligehausen, *et al.* 1983, Hayashi and Kokusho 1985).

Two different elements, namely the bond-link element and the bond-zone element, have been proposed to date for inclusion of the bond-slip effect in the finite element analysis of RC structures (De Groot, *et al*. 1981, Ngo and Scordelis 1967). However, the use of these elements requires a double node to represent the relative slip between reinforcing steel and concrete. In a beam structure defined by both end nodes along the direction, it is impossible to use the double node at each end node. To address this limitation in adopting the bond model, a numerical algorithm that includes the bond-slip effect in the moment-curvature relation is proposed in this study.

Unlike the critical region located in the vicinity of the beam mid-span, as well as at the ends of long-span beams, the behavior of the critical region at the beam-column joint of relatively short-span beams may be greatly affected both by the shear and also by the details of anchoring the beam reinforcement. In particular, slippage of the main bars from the anchorage zone (Δ_{total} in Fig. 8(a)) accompanies the rotation of the beam fixed-end, θ_{FE}. This cannot be simulated by any mechanical model, and the rigid body deformation, which accounts for approximately 50% of the total deformation (Saatcioglu and Ozcebe 1989), may increase as the deformation increases. This phenomenon will be enlarged in the case of an under-reinforced concrete beam. Consequently, its exclusion may

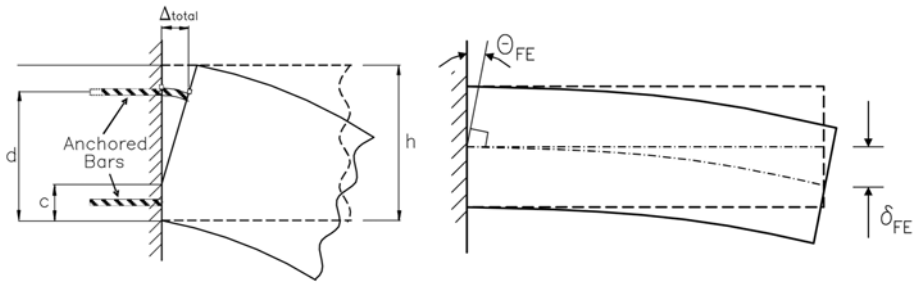

Fig. 8 Rigid body deformation at the beam-column joint

lead to an over-estimation of both the stiffness and the energy absorption capacity of the structure. Accordingly, to simulate the structural behavior more exactly, it is necessary to take into account the fixed-end rotation caused by the anchorage slip.

The anchorage slip Δ_{total} at a beam-column joint can be divided into two slip components according to the difference in the bond-slip behavior; Δ_{axial} induced from pull-out of the anchored reinforcement embedded through a column at beam-column joint and/or footing at column-footing joint and $\Delta_{bending}$ accompanied by the enlargement of bending cracks at the end face of a beam. Since Δ_{axial} and $\Delta_{bending}$ are basically caused by the axial force and bending moment, respectively, the anchorage slip Δ_{total} can be found by superposition of Δ_{axial} and $\Delta_{bending}$ after separate calculation of each slip component.

$$\Delta_{total}=\Delta_{axial}+\Delta_{bending} \tag{1}$$

4.3. Calculation of bond-slip component Δ_{axial}

A part of an RC member subjected to uniaxial tension is shown in Fig. 9. When the axial load P_h is applied, the far ends represent a fully cracked state with a steel strain of ε_{sl}, which means there is no load carrying by concrete. In advance, the tensile force P_h is transferred from the steel bar to the concrete by bond stress, and the value of the bond stress is zero at the inner end of the transfer length l_d. This means that there is no bond-slip at the central position. Moreover, it can be assumed that the strains in steel and concrete are equal to each other at $x=0$, and the strain value corresponds to ε_{s0}.

From the strain distribution, the local slip Δ_x can be defined as the total difference in elongation between the reinforcement and the concrete matrix measured over the length to a distance x from the mid-span.

$$\Delta_x = \int_0^x (\varepsilon_{sx}-\varepsilon_{cx})dx \tag{2}$$

where ε_{sx} and ε_{cx} are the strain distributions of steel and concrete, respectively (see Fig. 9).

On the basis of force equilibrium and the relation of Eq. (2) with the assumption that local bond stress is linearly dependent on the local slip, the following well-known governing differential equation for bond-slip can be obtained.

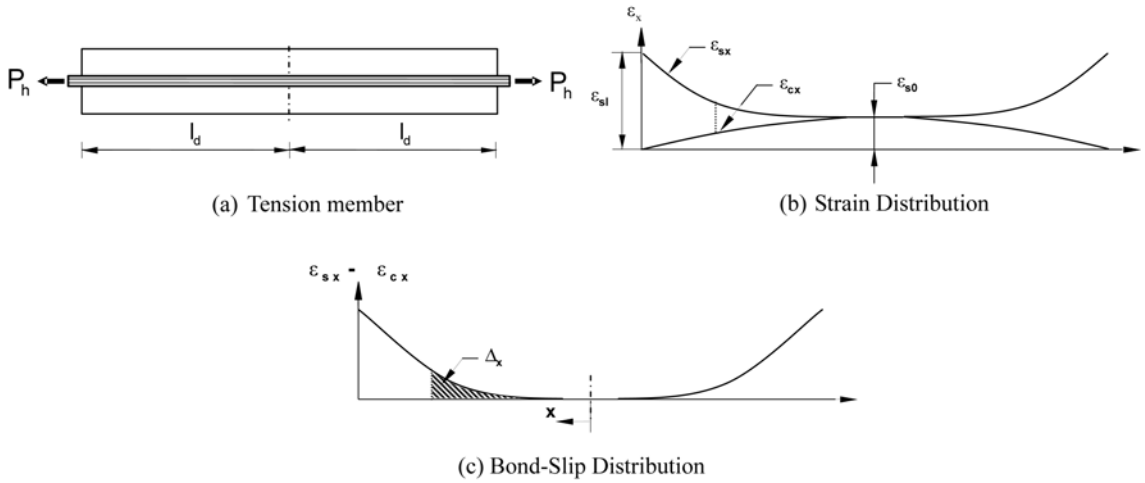

(a) Tension member (b) Strain Distribution

(c) Bond-Slip Distribution

Fig. 9 Behavior of tension member

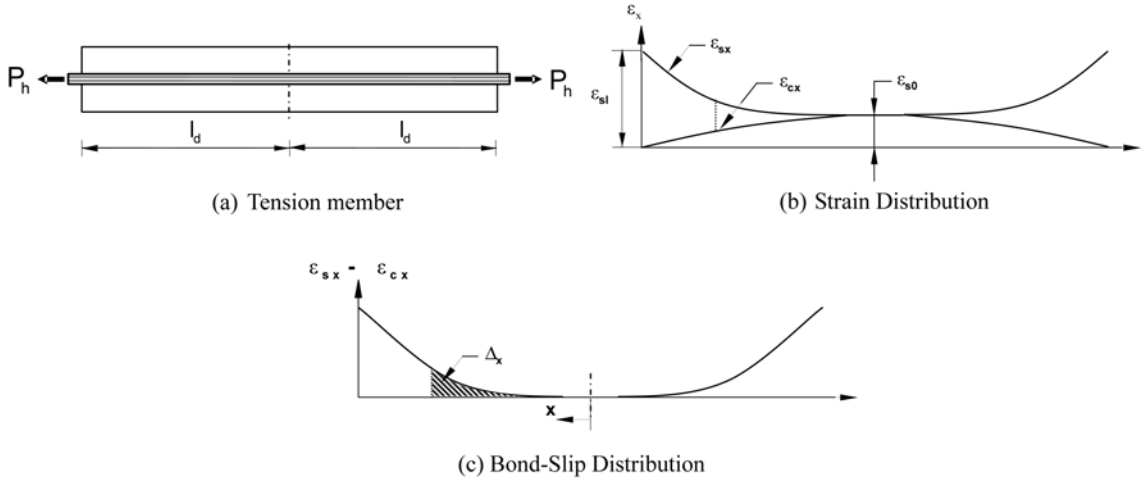

(a) Tension member (b) Strain Distribution

(c) Bond-Slip Distribution

Fig. 10 Embedded steel in RC column

$$\frac{d^2\Delta_x}{dx^2}-\frac{E_b\Sigma_0(1+\eta\rho)}{A_sE_s}\Delta_x=\frac{d^2\Delta_x}{dx^2}-k_1^2\Delta_x=0 \tag{3}$$

where $\eta=E_s/E_c$, the steel ratio $\rho=A_s/A_c$, Σ_0 is the perimeter of the steel bar, E_b is the slope of the bond stress-slip relation, and E and A mean elastic modulus and sectional area, respectively.

The general solution of Eq. (3) is given by $\Delta_x=C_1\sinh k_1x+C_2\cosh k_1x$, where C_1 and C_2 are constants that have to be determined from the boundary conditions. Focusing on the hooked anchorage of reinforcing bars in Fig. 10, bond slip represents the maximum value at the point where the bar enters the column at beam-column joint and/or footing at column-footing joint and slight bond slip may also occur at the starting point of the straight portion in front of the hook. If the bond-slip at the starting point of the straight portion in front of the hook is assumed to be Δ_0, then the constant C_2 will be Δ_0. In advance, as shown in Fig. 9(b), the strain difference at the column face that represents the maximum value can be determined from $d\Delta_x/dx=\varepsilon_{sx}-\varepsilon_{cx}$ by substituting the

anchorage length l_d into x:

$$\frac{d\Delta}{dx}(x=l_d)=k_1C_1\cosh(k_1l_d)+k_1\Delta_0\sinh(k_1l_d)=\varepsilon_{sl}-\varepsilon_{cl} \tag{4}$$

Since the concrete strain ε_c is negligibly small, compared with the steel strain, the other constant C_1 can be calculated as $C_1=(\varepsilon_{sl}-k_1\Delta_0\sinh(k_1l_d))/(k_1\cosh(k_1l_d))$. Accordingly, the general solution is finally determined, and the steel strain at $x=0$ can be computed as:

$$\varepsilon_{s0}=\frac{d\Delta}{dx}(x=0)=\frac{\varepsilon_{sl}}{\cosh(k_1l_d)}-\Delta_0k_1\tanh(k_1l_d) \tag{5}$$

The behavior of hooked bars in tension was studied experimentally by Soroushian, *et al.* (1988). They proposed the following relation between the tensile force (P_h) and the slip Δ_0 at the starting point of the hook ($x=0$) on the basis of experimental observations:

$$P_h=E_s\varepsilon_{s0}A_s=P_{hu}\left(\frac{\Delta_0}{2.54}\right)^{0.2},\quad P_{hu}=271(0.05d_b-0.25) \tag{6}$$

where the force term P_h is in kN, and the slip Δ_0 and bar diameter d_b are in mm.

Now the slip of anchored reinforcement, Δ_{axial}, can be calculated by substituting Δ_0 determined from Eqs. (5) and (6) into the general solution. The slip when the reinforcement yields at the column face ($x=l_d$) can finally be represented by

$$\Delta_{axial}=\frac{\varepsilon_{sy}}{k_1}\tanh(k_1l_d)+\frac{\Delta_0}{\cosh(k_1l_d)} \tag{7}$$

In the case of interior beam-column joint in which anchorage length l_d is enough and/or beams at both sides are bended symmetrically with respect to interior beam-column joint, Δ_{axial} can be assumed as zero. Therefore, it is necessary to calculate Δ_{axial} and Eq. (7) can be simplified as

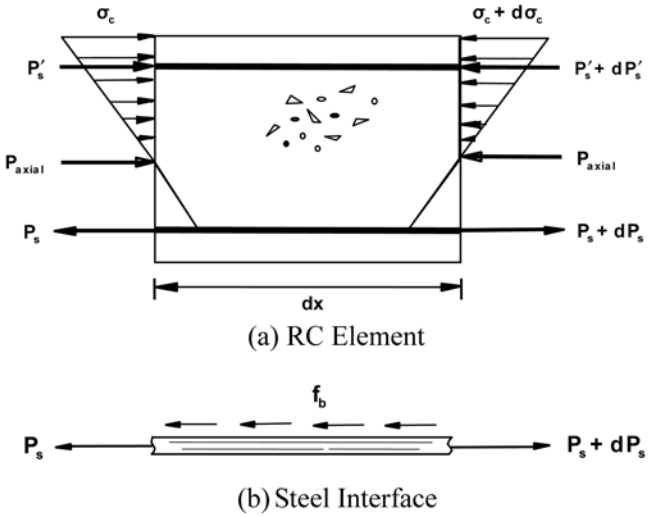

Fig. 11 Free body diagram for RC element

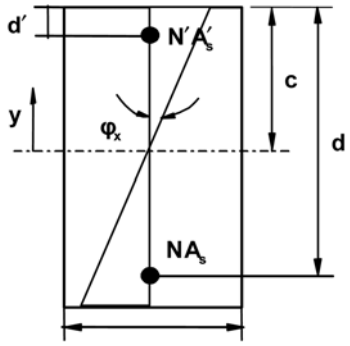

Fig. 12 Section geometry

$$\Delta_{axial} = \frac{\varepsilon_{sy}}{k_1}\tanh(k_1 l_d) \tag{8}$$

4.4. Calculation of bond-slip component $\Delta_{bending}$

Fig. 11 shows an infinitesimal beam element of length dx with axial force. If the linear bond stress-slip relation is assumed as shown in Fig. 4, the variations of the axial force components of steel located at the tension (dP_s) and compression (dP_s' region can be represented by Kwak and Kim (2002c):

$$dP_s = f_b \cdot dx \cdot \Sigma_0 = E_b \cdot \Delta \cdot dx \cdot \Sigma_0 = NA_s \cdot E_s \cdot d\varepsilon_s \tag{9}$$

$$dP_s' = N'A_s' \cdot E_s' \cdot d\varepsilon_s' = N'A_s' \cdot E_s'(c-d')d\phi_x \tag{10}$$

where N is the number of steels, f_b is the bond-stress at the steel interface and $(\,)'$ denotes the properties of steel in the compression part (see Fig. 12). Since the longitudinal strains are directly proportional to the distance from the neutral axis of zero strain, the variation of curvature ϕ_x representing the gradient of the strain profile at the section is also the variation of strain.

Until the reinforcing steel reaches its yielding stress, the concrete strain at the extreme compression fiber is not large enough to assume that the elastic modulus of concrete E_c is constant across the concrete section. By ignoring the tensile force in the concrete, which makes a negligibly small contribution after cracking, the variation of compression force of concrete in terms of curvature ϕ_x can be determined as:

$$dP_c = \int E_c d\varepsilon_c dA_c = \int_0^c E_c \cdot d\phi_x \cdot y \cdot b dy = E_c \cdot b \cdot d\phi_x \cdot \frac{1}{2}c^2 \tag{11}$$

where b is the width of section, and c is the distance from the extreme compression fiber to the neutral axis. Namely, the variation of curvature along the length can be expressed by $d\phi_x / dx = E_b \cdot \Sigma_0 \cdot \Delta_x / (E_c \cdot bc^2/2 + A_s' E_s' (c-d'))$ on the basis of the force equilibrium condition, $dP_c + dP_s' = dP_s$ (see Fig. 11)). The variation of concrete strain at the steel location can be simplified in terms of curvature ϕ_x as $d\varepsilon_c / dx = (d-c) \cdot d\phi_x / dx$.

When the bond-slip Δ_x at the steel-concrete interface is defined by the relative displacement between reinforcing steel and concrete ($\Delta = u_s - u_c$), the first order and second order differential equations of bond-slip lead to:

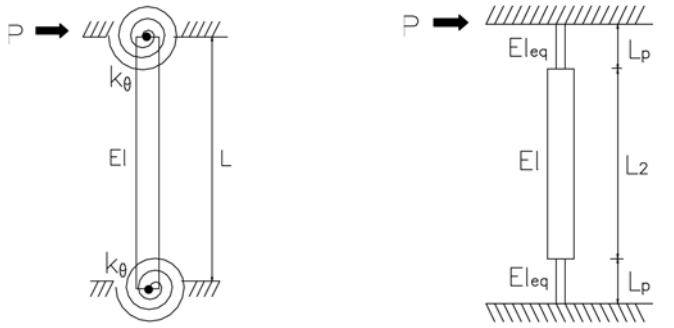

(a) Simplified Model with k_θ (b) Simplified Model with EI_{eq}

Fig. 13 Consideration of the equivalent stiffness

$$\frac{d\Delta_x}{dx} = \frac{du_s}{dx} - \frac{du_c}{dx} = \varepsilon_s - \varepsilon_c \tag{12}$$

$$\frac{d^2\Delta_x}{dx^2} = \frac{d\varepsilon_x}{dx} - \frac{d\varepsilon_c}{dx} = \frac{4E_b}{E_s d_s}\left\{1 - \frac{1-\alpha}{\frac{\alpha^2}{2\eta\rho} + \beta\left(\alpha - \frac{d'}{d}\right)}\right\}\Delta_x = k_1^2(1-\gamma)\Delta_x \tag{13}$$

where $\eta = \frac{E_s}{E_c}$, $\rho = \frac{NA_s}{bd}$, $\beta = \frac{N'A_s'E_s'}{NA_sE_s}$, $\alpha = \frac{c}{d}$.

Accordingly, the following governing differential equation for the bond-slip, which has the same form for an axial member (see Eq. 3), is obtained.

$$\frac{d^2\Delta_x}{dx^2} - k_2^2\Delta_x = 0 \tag{14}$$

The general solution to Eq. (14) is given by $\Delta_x = C_3\sinh k_2 x + C_4\cosh k_2 x$, in which C_3 and C_4 are constants that have to be determined from the boundary conditions, and k_2^2 means $k_1^2(1-\gamma)$. For a beam structure, it can be assumed that the steel and concrete strains at the end of a structure ($x=0$) are zero, because the bending moment by the applied lateral loads is zero. From the boundary condition of $d\Delta/dx(x=0) = \varepsilon_{s0} - \varepsilon_{c0} \cong 0$, a constant C_3 is consequently determined as zero. The constant C_4 can also be determined from the boundary condition of, $d\Delta/dx(x=l) = C_4k_2\sinh(k_2l) = \varepsilon_{sl} - \varepsilon_{cl} = \varepsilon_{sl} - (d-c)\phi_l$, where ϕ_l denotes the curvature at $x=l$ and can be calculated on the basis of the force equilibrium of $P'_{cl} + P'_{sl} = P_{sl} + P_{axial}$ at the beam-column joint, in which P_{axial} is the applied axial load. Finally, the bond-slip induced from the bending behavior, $\Delta_{bending}$, is represented by:

$$\Delta_{bending} = C_4\cosh(k_2l) = \frac{(1-\gamma(1+\lambda))\varepsilon_{sy}}{k_2\sinh(k_2l)}\cosh(k_2l) = \frac{(1-\gamma(1+\lambda))\varepsilon_{sy}}{k_2\tanh(k_2l)} \tag{15}$$

where $\lambda = P_{axial}/P_{sl}$.

Since Eq. (15), however, includes an unknown variable γ(see Eq. (13)), the bond-slip is not directly determined. This means that the introduction of a formula related to the bond-slip is

required; a relation introduced by Gergely and Lutz (1973), being popularly used to determine the allowable crack width of cracked RC structures, is adopted in this study:

$$w_{\max} = 1.08\beta_c f_s \sqrt[3]{d_c A} \times 10^{-5} \ (mm) \tag{16}$$

where β_c is the ratio of distances from the tension face and from the steel centroid to the neutral axis, d_c is the thickness of the concrete cover, and A is the concrete area surrounding one bar.

Because it can be assumed that crack width w is equivalent to two times the bond-slip at the cracked location ($0.5w = \Delta_{bending}$), the unknown variable γ can be determined from Eqs. (15) and (16) with assumed β_c, which has a recommended value of 1.2 in a beam without axial force. Then, the neutral axis depth c is calculated from the relation of $r = (1-\alpha)/\{\alpha^2/2\eta\rho + \beta(\alpha - d'/d)\}$ in Eq. (13). In advance, β_c is recalculated and again compared with the assumed value, and these iterations are repeated until the difference between β_c assumed and calculated is less than the given tolerance. Generally, the neutral axis depth c decreases with an increase of the bending moment acting on a section. Nevertheless, a constant value of c determined on the basis of the yielding of reinforcing steel at the beam-column joint ($x = l$) is assumed as a representative constant value along the entire span length for the computational convenience, because the neutral axis depth maintains an almost constant value from the initial cracking up to the yielding of reinforcing steel and the behavior of the beam-column joint mainly affect the global behavior of the structures.

5. Calculation of equivalent stiffness

To account for the fixed-end rotation in this study, the reduced stiffness, EI, in the moment-curvature relation for the elements located at the ends of the beam within the range of the plastic hinge length L_p is used. Among the various empirical expressions have been proposed, in the case of no axial load, the relatively simple equation of $L_p = 0.25d + 0.075z$, proposed by Sawyer (1964), can effectively be used, where d and z are the effective depth of a section and the distance from the critical section to the point of contraflexure, respectively. However, since the plastic hinge length increases in proportion to the applied axial load, it may be difficult to estimate the plastic hinge length of an axially loaded member with only this simple equation. Accordingly, the plastic hinge length of $L_p = xh$, proposed by Bayrak and Sheikh (1997), is introduced as an upper limit value, where h is the section depth and x is an experimental parameter ranging from 0.9 to 1.0, and an inequality condition of $L_p \le d$ is designated in this paper for simplicity of analysis.

If a beam with rotational stiffness k_θ at both ends is subjected to a horizontal force P, as shown in Fig. 13(a), the corresponding horizontal drift Δ_1 in which shear deformations are being neglected for simplifying formulation can be obtained by

$$\Delta_1 = \frac{PL^3}{12EI} + \frac{PL^2}{2k_\theta} \tag{17}$$

where the first term is the contribution by the bending deformation of the beam and the second term by the end rotational stiffness k_θ. This rotational stiffness can be determined on the basis of Δ_{total} calculated by $\Delta_{total} = \Delta_{axial} + \Delta_{bending}$.

$$\theta_{fe} = \frac{\Delta_{total}}{d-c}, \quad k_\theta = \frac{M_y}{\theta_{fe,y}} \tag{18}$$

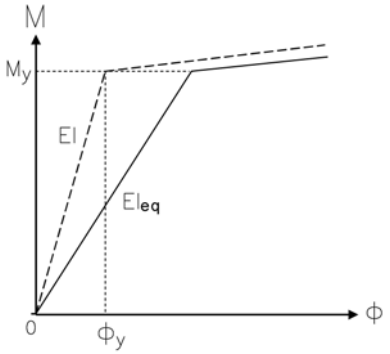

Fig. 14 Modification of monotonic envelope curve

where M_y is the moment and $\theta_{fe,y}$ is rigid body rotation at the beam-column joint when reinforcing steels yield, respectively.

When the same force acts on a beam with reduced stiffness EI_{eq} at both ends, as shown in (b), the horizontal deflection Δ_2 can also be calculated by the moment area method.

$$\Delta_2 = \frac{P\{EI_{eq}L_2^3 + 2EIl_p(4l_p^2 + 6l_pL_2 + 3L_2^3)\}}{12EI_{ep}EI} \tag{19}$$

From the equality condition of $\Delta_1 \equiv \Delta_2$, the equivalent stiffness EI_{eq} can be determined by

$$\frac{1}{EI_{eq}} = \frac{1}{\beta \cdot k_\theta \cdot L} + \frac{1}{EI} \tag{20}$$

where $\beta = \alpha(1 - 2\alpha + 4/3\alpha^2)$, $\alpha = L_p/L$.

The same derivation procedure for a cantilevered beam is applied and the equivalent stiffness EI_{eq} obtained in this case has the same form as Eq. (20) except the parameter β has the form of $\beta = \alpha(1 - \alpha + 1/3\alpha^2)$. The bending stiffness of elements located within the plastic hinge length L_p from both end faces of a member will be represented by EI_{eq} instead of EI which is still used at the other region. This means that the slope of moment-curvature relation is finally modified (see Fig. 14).

6. Solution algorithm

For the analysis of RC structures, Timoshenko beam theory was used in this study (Owen and Hinton 1980). This theory is well established and widely used in the analysis of beams, and details for the formulation of a beam element can be found elsewhere (Owen and Hinton 1980). In a typical Timoshenko beam, it is usual to assume that normal to the neutral axis before deformation remains straight, but this is not necessarily after deformation. In addition, the effects of shear deformations are not taken into consideration in simulating nonlinear behavior since the normal bending stresses reach a maximum at the extreme fibers, where the transverse shear stresses are at their lowest value, and reach a minimum at mid-depth of the beam, where the transverse shear stresses are highest. Thus, the interaction between transverse shear stresses and normal bending stresses is relatively small and can be ignored. This means that the flexural rigidity EI is replaced

Table 1 Material and sectional properties used in application

SPECIMEN	E_c (MPa)	E_s (MPa)	f_c (MPa)	f_y (MPa)	ρ (A_s/bd)	ρ' (A_{sc}/bd)	P (kN)
BEAMR6	24,804	200,569	31	451	0.014	0.014	0
BEAMR4	22,785	200,569	30	451	0.014	0.007	0
BEAMS1	27,770	200,569	34	496	0.012	0.012	0
COLUMN1	23,975	200,569	26	496	0.012	0.012	178
COLUMN2	30,447	200,569	42	496	0.010	0.010	45

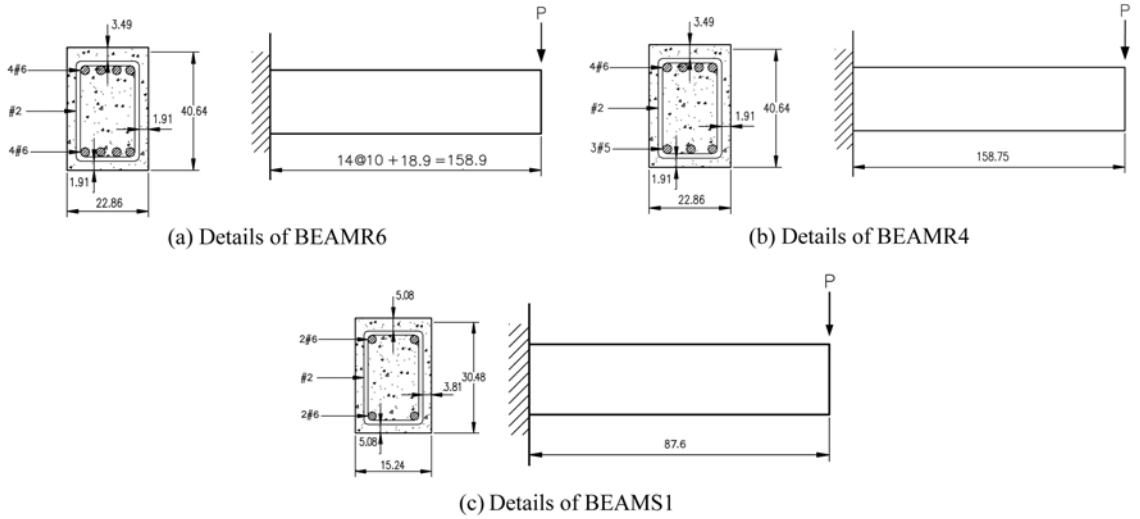

(a) Details of BEAMR6 (b) Details of BEAMR4

(c) Details of BEAMS1

Fig. 15 Details of beam members (unit: cm)

by that corresponding to the curvature calculated from the nodal displacements by $\phi=(\theta_i-\theta_j)/L$, whereas the shear rigidity of a beam element GA is assumed to be unchanged, where θ_i and θ_j denote the rotational deformations at both end nodes, and L is the element length. Every nonlinear analysis algorithm consists of four basic steps: formation of the current stiffness matrix, solution of the equilibrium equations for the displacement increments, state determination of all elements in the model, and a convergence check. Since the global stiffness matrix of the structure depends on the displacement increments, the solution of equilibrium equations is typically accomplished with an iterative method through the convergence check. The nonlinear solution scheme selected in this study uses a tangent stiffness matrix at the beginning of each load step in combination with a constant stiffness matrix during the subsequent correction phase; that is, the incremental-iterative method.

All the remaining algorithms, from the construction of an element stiffness matrix to the iteration at each load step, correspond with those used in a classical nonlinear analysis of RC structures. More details can be found elsewhere (Ayoub and Filippou 1999, Chen 1982, Hayashi and Kokusho 1985, Monti, *et al*. 1997).

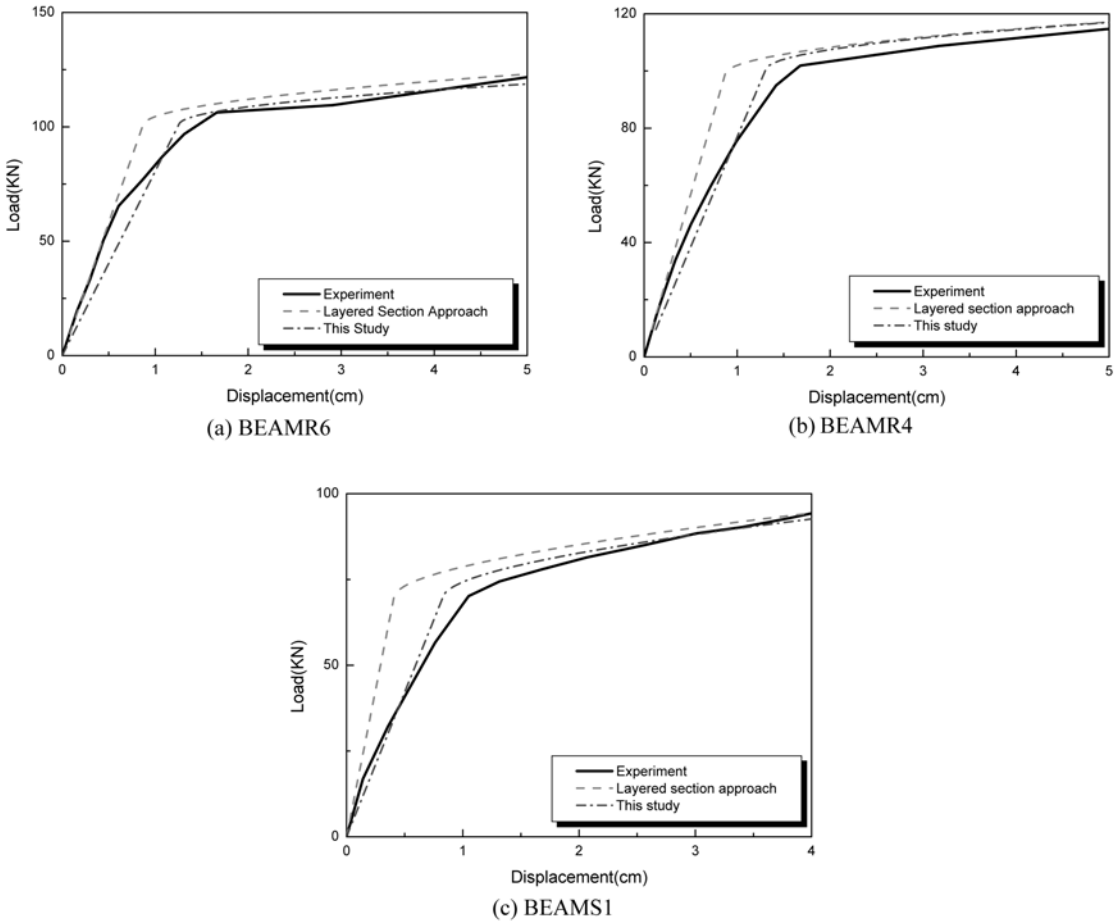

Fig. 16 Load-deflection relation for beam members

7. Numerical application

In order to establish the validity and applicability of the proposed moment-curvature relation, correlation studies between analytical results and experimental studies are conducted. Among the many experimental results available in the literature, five RC specimens are investigated and discussed, as these specimens represent typical structural behaviors according to various effects such as steel ratio, boundary condition, and application of axial force. These specimens are BEAMR6 and BEAMR4 experimented by Ma, *et al.* (1976), specimen 00.147 (BEAMS1) and 40.048 (COLUMN1) experimented by Wight and Sozen (1975), and specimen 1 (COLUMN2) experimented by Low and Moehle (1987). The material and sectional properties of each specimen are summarized in Table 1.

The geometry and cross-sectional dimensions of the three beam members are presented in Fig. 15. The first two specimens represent an isolated part of a girder near the exterior column connections, and bending mechanism is largely responsible for the structural behavior. On the other hand, the last specimen represent interior connection without hooked bar and the structural response of the this specimen appears to be affected more by shear force than the other beam specimens because of its

relatively small span to depth ratio. In these specimens, the plastic deformation is concentrated at the end of a beam with narrow width, accompanying fixed-end rotation that occurs in addition to elastic rotation at the cracking stage. To simulate more exact structural behavior with the beam element formulated on the basis of the average deformation in an element, a separate consideration of this region is required in the finite element modeling. This is necessary because the ultimate capacity may be overestimated if the plastic hinge length is not precisely taken into consideration. Since the calculated plastic hinge length L_p is determined as 20 cm for BEAMR6 and BEAMR4, and 15 cm for BEAMS1, the specimens are modeled along the entire span with an element of $L = 10$ cm except a right end element.

Fig. 16 compares the load deflection relations obtained by a layered section approach and the proposed model with the experimental results of BEAMR6, BEAMR4 and BEAMS1. The layered section approach gives very satisfactory predictions of the elastic behavior before initial cracking and of the value of yielding moment itself, but the displacements corresponding to the yielding moment are underestimated. This means that the layered section approach, which adopts a perfect bond assumption, is limited in terms of describing the cracking behavior of RC beams that are accompanied by a fixed-end rotation concentrated at the end of the beam. Larger differences from the experimental data are also expected when a RC beam is subjected to severe dynamic loading, such as seismic loads and wind loads because the slope of the subsequent inelastic unloading and reloading curves will be overestimated. These results indirectly explain why the fixed-end rotation

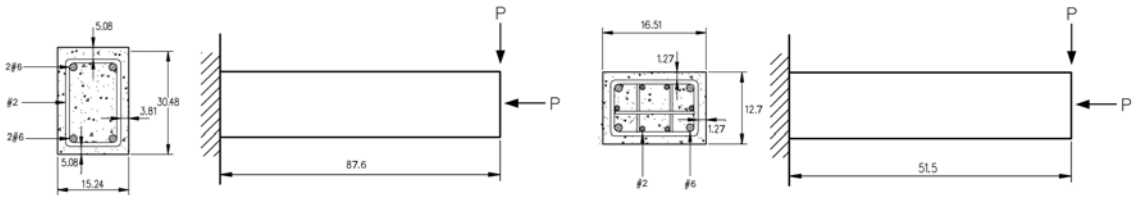

(a) COLUMN1 (b) COLUMN2

Fig. 17 Details of column members (unit: cm)

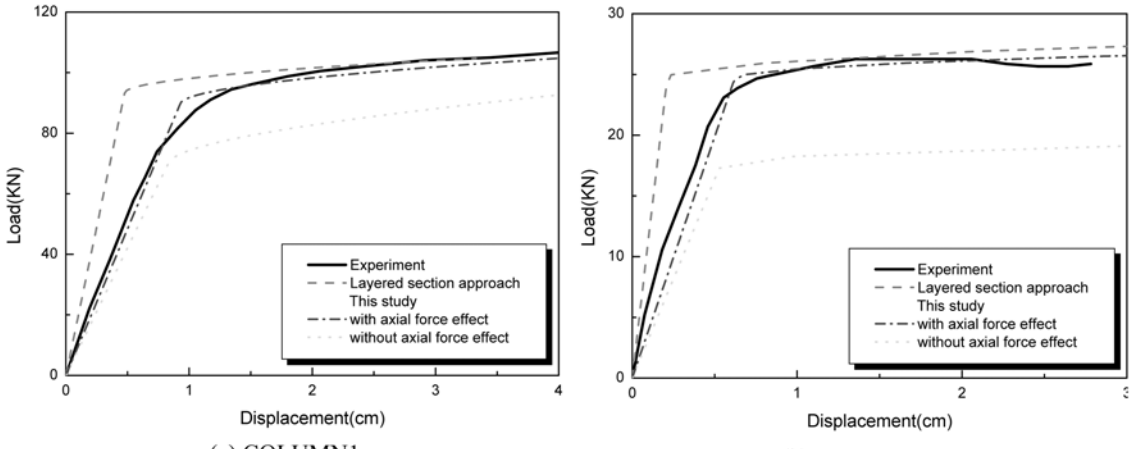

(a) COLUMN1 (b) COLUMN2

Fig. 18 Load-deflection relation for column members

effect must be considered.

In contrast, the introduced numerical model, which considers the fixed-end rotation effect according to the aforementioned modification procedure, provides good agreement with experimental results through the entire loading steps. The elastic stiffnesses before the initial cracking are underestimated because the fixed-end rotation is taken into account by changing the average bending stiffness *EI* without any further consideration of uncracked or cracked section states (see Fig. 14). However, these differences at the elastic loading steps do not represent a remarkable influence on the entire structural response ranging from initial cracking to large deformations after yielding of steel. In spite of relatively accurate consideration of the fixed-end rotation effect in the introduced numerical model, a slight difference between the analytical response and the experimental data still exist, because the introduced numerical model does not reflect the stiffness degradation caused by shear cracks accompanied with bending cracks. Nevertheless, the proposed model can effectively be used in simulating the nonlinear response of RC beams.

The next two specimens, COLUMN1 and COLUMN2, are selected to demonstrate additional effects by the axial load, and details of these specimens are presented in Fig. 17.

Since λ in Eq. (15) and β_c in Eq. (16) represent the different values as the axial load acts (λ=0.631, β_c=1.4 for COLUMN1, λ=0.484, β_c=1.24 for COLUMN2), $\Delta_{bending}$ calculated in Eq. (15) will be changed, and RC columns show different slip behavior from that of RC beams. In addition, the specimens are modeled along the entire span with an element of l=5 cm on the basis of the plastic hinge length, excluding a right end element.

The responses represented in Fig. 18 compare the load deflection relations obtained by the layered section approach and the proposed model with the experimental results. The results of the present study display very satisfactory agreement with the measured data. Meanwhile, the numerical results not considering the axial force effect represent an underestimation of the stiffness and the ultimate strength of RC columns. These differences will be enlarged as the magnitude of the axial load increases. Finally, the proposed analytical method can also be effectively used to calculate the nonlinear behavior of RC columns subject to axial load as well as RC beams without axial force.

8. Conclusions

This paper concentrates on the introduction of nonlinear analysis of RC beams and columns based on simplified moment-curvature relations. Unlike most mathematical or mechanical models found in the literature, the proposed model has taken into account fixed-end rotation caused by anchorage slip at the fixed-end of a beam-column joint. Also, to consider axial force effect, the basic moment-curvature relation of the section which is uniquely defined according to the dimensions of the concrete section and the material properties of concrete and steel and axial force is modified. The efficiency and reliability of the proposed model are demonstrated by comparison between experimental data and numerical results. Additional consideration of the strength degradation under cyclic loading beyond the yield strength should be required to estimate the exact damage level undergone by a section after a certain number of cycles.

Correlation studies between analytical results and experimental values for the representative RC beams and columns have yielded the following conclusions : (1) to accurately predict the structural behavior of an RC beam-to-column sub-assemblage where the nonlinear response is concentrated, a modification of the moment-curvature relation is strongly required to consider fixed end rotation

caused by anchorage slip; (2) to effectively simulate axially loaded RC columns, additional modification of the moment-curvature relation is strongly required; and finally (3) the proposed model can be effectively used as an envelope curve in defining the hysteretic behavior of RC beams and columns.

References

Assa, B. and Nishiyama, M. (1998), "Prediction of load-displacement curve of high-strength concrete columns under simulated seismic loading", *ACI Struct. J.*, **95**(5), 547-557.

Ayoub, A. and Filippou, F. C. (1999), "Mixed formulation of bond-slip problems under cyclic loads", *J. Struct. Eng.*, **125**(6), 661-671.

Bayrak, O. and Sheikh, S. A. (1997), "High-strength concrete columns under simulated earthquake loading", *ACI Struct. J.*, **94**(6), 708-722.

Chen, W. F. (1982), *Plasticity in Reinforced Concrete*, McGraw-Hill Book Company.

Clough, R. W. and Johnston, S. B. (1966), "Effect of stiffness degradation on earthquake ductility requirements", *Proceedings of Japan Earthquake Engineering Symposium*, October.

De Groot, A. K., Kusters, G. M. A. and Monnier, T. (1981), "Numerical modeling of bond-slip behavior", *Concrete Mech.*, **26**(1B), 6-38.

Dowell, R. K., Seible, F. and Wilson, E. L. (1998), "Pivot hysteresis model for reinforced concrete members", *ACI Struct. J.*, **95**(5), 607-617.

Eligehausen, R., Popov, E. P. and Bertero, V. V. (1983), "Local bond stress-slip relationships of deformed bars under generalized excitations", Report No. UCB/EERC 83-23. Earthquake Engineering Research Center, University of California, Berkeley.

Gergely, P. and Lutz. L. A. (1973), "Maximum crack width in reinforced concrete flexural members", *ACI Special Publication SP-20*, 87-117.

Hayashi, S. and Kokusho, S. (1985), "Bond behavior in the neighborhood of the crack", *Proceedings of the U.S.-Japan Joint Seminar on Finite Element Analysis of Reinforced Concrete*, Tokyo, 364-373.

Keshavarzian, M. and Schnobrich, W. C. (1984), "computed nonlinear seismic response of R/C wall-frame structures", *Structural Research Series* No. 515, University of Illinois, Urbana, IL.

Kwak, H. G., and Filippou, F. C. (1990), "Finite element analysis of reinforced concrete structures under monotonic loads", Report No. UCB/SEMM-90/14, Structural Engineering Mechanics and Materials, University of California, Berkeley, CA.

Kwak, H. G., Kim, S.-P. and Kim, J.-E. (2004), "Nonlinear dynamic analysis of RC frames using cyclic moment-curvature relation", *Struct. Eng. Mech.*, **17**(3-4), 357-378.

Kwak, H. G., Kim, J. H. and Kim, S. H. (2006), "Nonlinear analysis of prestressed concrete structures considering slip behavior of tendons", *Comput. Concrete*, **3**(1), 43-64.

Kwak, H. G. and Kim, S. P. (2001), "Nonlinear analysis of RC beams subject to cyclic loadings", *J. Struct. Eng.*, ASCE, **127**(12), 1436-1444.

Kwak, H. G. and Kim, S. P. (2002a), "Cyclic moment-curvature relation of RC beam", *Mag. Concrete Res.*, **54**(6), 435-447.

Kwak, H. G. and Kim, S. P. (2002b), "Monotonic moment-curvature relation of RC beam", *Mag. Concrete Res.*, **54**(6), 423-434.

Kwak, H. G. and Kim, S. P. (2002c), "Nonlinear analysis of RC beams based on moment-curvature Relation", *Comput. Struct.*, **80**(6), 615-628.

Low, S. S. and Moehle, J. P. (1987), "Experimental study of reinforced concrete columns subjected to multi-axial cyclic loading", Earthquake Engingeering Research Center Report No. EERC 87-14, University of California, Berkeley, CA.

Ma, S. M., Bertero, V. V. and Popov, E. P. (1976), "Experimental and analytical studies on the hysteretic behavior of reinforced concrete rectangular and T-Beam", Earthquake Engineering. Research Center Report No. EERC 76-2, University of California, Berkeley, CA.

Monti, G., Filippou, F. C. and Spacone, E. (1997) "Analysis of hysteretic behavior of anchored reinforcing bars", *ACI Struct. J.*, **94**(2), 248-261.
Monti, G., Filippou, F. C. and Spacone, E. (1997) "Finite element for anchored bars under cyclic load reversals", *J. Struct. Eng.*, **123**(5), 614-623.
Ngo, D. and Scordelis, A. C. (1967) "Finite element analysis of reinforced concrete beams", *ACI J.*, **64**(3), 152-163.
Owen, D. R. J. and Hinton, E. (1980) *Finite Elements in Plasticity*, Pineridge Press Limited.
Park, R., Kent, D. C. and Sampson, R. A. (1972) "Reinforced concrete members with cyclic loading", *J. Struct. Div.*, ASCE, **98**(ST7), 1341-1360.
Park, R. and Paulay, T. (1975) *Reinforced Concrete Structures*, John Wiley & Sons.
Roufaiel, M. S. L. and Meyer, C. (1987) "Analytical modeling of hysteretic behavior of reinforced concrete frame", *J. Struct. Eng.*, **113**(3), 429-444.
Saatcioglu, M. and Ozcebe, G. (1989) "Response of reinforced concrete columns to simulated seismic loading", *ACI Struct. J.*, **86**(1), 3-12.
Sawyer, H. A. (1964) "Design of concrete frames for two failure states", *Proceedings of the International Symposium on the Flexural Mechanics of Reinforced Concrete*, ASCE-ACI, Miami, November, 405-431.
Scott, B. D., Park, R. and Priestley, M. J. N. (1982), "Stress-strain behavior of concrete confined by overlapping hoops at low and high strain rates", *ACI J.*, **79**(1), 13-27.
Soroushian, P., Obaseki, K., Nagi, M. and Rojas, M. (1988) "Pullout behaviour of hooked bars in exterior beam-column connections", *ACI Struct. J.* **85**(3), 269-276.
Takeda, T., Sozen, M. A. and Nielsen, N. N. (1970) "Reinforced concrete response to simulated earthquake", *J. Struct. Div.*, ASCE, **96**(12), 2257-2573.
Taucer, T., Spacone, E. and Filippou, F. C. (1991), "A fiber beam-column element for seismic response analysis of reinforced concrete structures", *Earthquake Engineering. Research Center Report* No. EERC 91-17, University of California, Berkeley, CA.
Wight, J. K. and Sozen, M. A. (1975) "Strength decay of RC columns under shear reversals", *J. Struct. Div., ASCE*, **101**(ST-5), 1053-1065.

CC